Cyclopentadienone Iron Alcohol Complexes: Synthesis, Reactivity, and Implications for the Mechanism of Iron Catalyzed Hydrogenation of Aldehydes

Charles P. Casey* and Hairong Guan

Department of Chemistry, University of Wisconsin-Madison,

Madison, Wisconsin 53706

casey@chem.wisc.edu

Supporting Information

Contents:

General Experimental Information. All air-sensitive compounds were prepared and handled under a nitrogen atmosphere using standard Schlenk and inert-atmosphere box techniques. Toluene was deoxygenated and dried in a solvent purification system by passing through an activated alumina column and an oxygen-scavenging column under nitrogen.[1] CD_2Cl_2 was dried over CaH_2 and distilled under nitrogen. Toluene-d_8 was distilled from Na and benzophenone under nitrogen. {2,5-$(SiMe_3)_2$-3,4-[$(CH_2)_4$](η^5-C_4COH)}$Fe(CO)_2H$ (**3**),[2] {2,5-$(SiMe_3)_2$-3,4-[$(CH_2)_4$](η^4-C_4CO)}$Fe(CO)_3$ (**10**),[3] 4-$HOCH_2C_6H_4CHO$ (**11**),[4] and 4-$(CHO)C_6H_4CH(OCH_3)_2$[5] were prepared as described in the literature.

Synthesis of Alcohol Complexes. For the convenience of compound characterization, alcohol complexes were generated *in situ* by mixing equimolar amounts of hydride **3** (12 μmol) and an aldehyde (12 μmol) in 500 μL of CD_2Cl_2 (or toluene-d_8) in a resealable NMR tube for 10 min at room temperature. NMR spectra of the orange alcohol complex solutions[6] were obtained in an NMR probe cooled to 0 °C. Infrared spectra of the alcohol complexes (in toluene) were taken in a CaF_2 solution cell at room temperature.

{2,5-$(SiMe_3)_2$-3,4-[$(CH_2)_4$](η^4-C_4CO)}$Fe(CO)_2$(*p*-$CH_3C_6H_4CH_2OH$) (6-CH_3). ^{1}H NMR (CD_2Cl_2, 360 MHz, 0 °C) δ 0.20 (s, $Si(CH_3)_3$, 18H), 1.07 (br s, OH, 1H), 1.23-1.37 (m, CH_2, 2H), 1.42-1.56 (m, CH_2, 2H), 1.97-2.16 (m, CH_2, 4H), 2.35 (s, ArCH_3, 3H), 4.48 (s, ArCH_2OH, 2H), 7.18-7.28 (m, Ar, 4H). ^{1}H NMR (toluene-d_8, 360 MHz, 0 °C) δ 0.39 (s, $Si(CH_3)_3$, 18H), 0.97-1.13 (m, CH_2, 4H), 1.38 (s, OH, 1H), 1.78-1.89 (m, CH_2, 2H), 1.91-2.04 (m, CH_2, 2H), 2.06 (s, ArCH_3, 3H), 4.16 (s, ArCH_2OH, 2H), 6.92-7.12 (m, Ar, 4H). ^{13}C{^{1}H} NMR (CD_2Cl_2, 90 MHz, 0 °C) δ 0.28 ($Si(CH_3)_3$), 21.44 (CH_3), 22.29 (CH_2), 24.83 (CH_2), 73.60 ($ArCH_2OH$), 75.44, 107.34, 128.80 (CH), 129.59 (CH), 135.32, 139.04, 171.18 (C=O), 212.71 ($Fe(CO)_2$). ^{13}C{^{1}H} NMR (toluene-d_8, 90 MHz, 0 °C) δ 0.41 ($Si(CH_3)_3$), 22.03 (CH_2), 24.71 (CH_2), 73.12 ($ArCH_2OH$),

75.52, 107.16, 129.47 (CH), 135.14, 138.49, 171.76 (C=O), 212.83 ($Fe(CO)_2$); tolyl CH_3 and one aromatic carbon resonance were not located. IR (toluene) 2012, 1959 cm^{-1}.

{2,5-$(SiMe_3)_2$-3,4-[$(CH_2)_4$](η^4-C_4CO)}$Fe(CO)_2$(*p*-$NO_2C_6H_4CH_2OH$) (6-NO_2). ^1H NMR (CD_2Cl_2, 360 MHz, 0 ˚C) δ 0.22 (s, $Si(CH_3)_3$, 18H), 1.20-1.32 (m, CH_2, 2H), 1.42-1.55 (m, CH_2, 2H), 1.95-2.16 (m, CH_2, 4H), 4.65 (s, $ArCH_2OH$, 2H), 7.50 (d, *J* = 8.6 Hz, Ar, 2H), 8.24 (d, *J* = 8.6 Hz, Ar, 2H), OH resonance was not located. ^1H NMR (toluene-d_8, 360 MHz, 0 ˚C) δ 0.36 (s, $Si(CH_3)_3$, 18H), 0.95-1.16 (m, CH_2, 4H), 1.26 (br s, OH, 1H), 1.75-1.88 (m, CH_2, 2H), 1.89-1.97 (m, CH_2, 2H), 3.96 (s, $ArCH_2OH$, 2H), 6.80 (d, J = 7.9 Hz, Ar, 2H), 7.74 (d, *J* = 7.9 Hz, Ar, 2H). $^{13}C\{^1H\}$ NMR (CD_2Cl_2, 90 MHz, 0 ˚C) δ 0.32 ($Si(CH_3)_3$), 22.20 (CH_2), 24.77 (CH_2), 72.61 ($ArCH_2OH$), 76.41, 107.87, 124.26 (CH), 129.07 (CH), 145.32, 148.18, 170.27 (C=O), 212.40 ($Fe(CO)_2$). $^{13}C\{^1H\}$ NMR (toluene-d_8, 90 MHz, 0 ˚C) δ 0.38 ($Si(CH_3)_3$), 21.93 (CH_2), 24.62 (CH_2), 72.19 ($ArCH_2OH$), 76.46, 107.74, 123.73 (CH), 128.31 (CH), 144.17, 148.04, 170.85 (C=O), 212.53 ($Fe(CO)_2$). IR (toluene) 1999, 1940 cm^{-1}.

{2,5-$(SiMe_3)_2$-3,4-[$(CH_2)_4$](η^4-C_4CO)}$Fe(CO)_2$(*p*-$CH_3OC_6H_4CH_2OH$) (6-OCH_3). ^1H NMR (CD_2Cl_2, 360 MHz, 0 ˚C) δ 0.19 (s, $Si(CH_3)_3$, 18H), 0.98 (br s, OH, 1H), 1.23-1.35 (m, CH_2, 2H), 1.42-1.55 (m, CH_2, 2H), 1.97-2.15 (m, CH_2, 4H), 3.80 (s, OCH_3, 3H), 4.45 (s, $ArCH_2OH$, 2H), 6.90 (d, *J* = 8.6 Hz, Ar, 2H), 7.25 (d, *J* = 8.6 Hz, Ar, 2H). $^{13}C\{^1H\}$ NMR (CD_2Cl_2, 90 MHz, 0 ˚C) δ 0.28 ($Si(CH_3)_3$), 22.29 (CH_2), 24.83 (CH_2), 55.66 (OCH_3), 73.15 ($ArCH_2OH$), 75.36, 107.30, 114.14 (CH), 130.49, 130.53 (CH), 160.29, 171.24 (C=O), 212.72 ($Fe(CO)_2$). IR (toluene) 1998, 1938 cm^{-1}.

{2,5-$(SiMe_3)_2$-3,4-[$(CH_2)_4$](η^4-C_4CO)}$Fe(CO)_2$(*p*-$CF_3C_6H_4CH_2OH$) (6-CF_3). ^1H NMR (CD_2Cl_2, 360 MHz, 0 ˚C) δ 0.22 (s, $Si(CH_3)_3$, 18H), 1.21-1.36 (m, CH_2, 2H), 1.42-1.56 (m, CH_2, 2H), 1.79 (br s, OH, 1H), 1.95-2.16 (m, CH_2, 4H), 4.60 (s, $ArCH_2OH$, 2H), 7.46 (d, J = 7.9 Hz,

Ar, 2H), 7.66 (d, J = 7.9 Hz, Ar, 2H). $^{13}C\{^1H\}$ NMR (CD_2Cl_2, 90 MHz, 0 °C) δ 0.31 ($Si(CH_3)_3$), 22.23 (CH_2), 24.81 (CH_2), 72.96 ($ArCH_2OH$), 76.10, 107.68, 125.06 (q, $^1J_{C\text{-}F}$ = 365.7 Hz, CF_3), 125.98 (q, $^3J_{C\text{-}F}$ = 3.8 Hz, CH), 128.84 (CH), 125.06 (q, $^2J_{C\text{-}F}$ = 32.3 Hz, *C*CF_3), 142.26, 170.54 (C=O), 212.48 ($Fe(CO)_2$). IR (toluene) 1999, 1940 cm^{-1}.

{2,5-$(SiMe_3)_2$-3,4-[$(CH_2)_4$](η^5-C_4COD)}$Fe(CO)_2$D (3-*d*$_2$) was prepared in 75 % yield from the reaction between the solution of iron tricarbonyl complex **10** in THF and 40 wt % of NaOD (in D_2O), followed by the addition of 85 wt % of D_3PO_4 (in D_2O).[7] The isolated **3-*d*$_2$** contained 95 % deuterium at both OD and FeD positions.

^{2}H NMR Study of the Stoichiometric Reduction of Benzaldehyde by 3-*d*$_2$. A solution of **3-*d*$_2$** (15.8 mg, 40 μmol) in toluene (400 μL) in a Teflon capped NMR tube was frozen in a liquid nitrogen bath. The frozen solution was layered with 100 μL of toluene first, and then with a frozen solution of PhCHO (8.0 μL, 80 μmol) in toluene (100 μL). The mixture was thawed in a dry ice/acetone bath and the three layers were carefully mixed while cold. The NMR tube was then immediately inserted into an NMR spectrometer precooled to –30 ºC. The progress of reduction was monitored by ^{2}H NMR spectroscopy. After 20 min, the reaction was complete and two peaks (δ 1.37 and 4.03) corresponding to coordinated PhCHDOD were seen. When the solution was warmed to 0 ºC, a resonance for the dissociated alcohol was observed at δ 4.54. When the temperature was further raised to 10 ºC, the characteristic aldehyde peak (δ 9.70) for PhCDO was observed.

Attempted Kinetic Study on Benzaldehyde Reduction by 3. A solution **3** (1.8 mg, 4.5 μmol) in toluene-d_8 (450 μL) in a Teflon capped NMR tube was frozen in a liquid nitrogen bath, and a solution of PhCHO (5.1 μL, 50 μmol) in toluene (50 μL) was added via a gas tight syringe through the Teflon cap. The mixture was thawed in a dry ice/acetone bath and the two layers

were carefully mixed while cold. The NMR tube was then immediately inserted into an NMR spectrometer precooled to –72 °C. The first spectrum, recorded within 3 min, showed that about 80 % of **3** had reacted. The disappearance **3** was followed as a function of time, and the observed rate constant was estimated with great error.

Exchange Reactions between 3 and D_2 and between 3 and ^{13}CO. A solution of **3** (7.8 mg, 20 μmol) in 500 μL of toluene-d_8 in a J. Young high pressure NMR tube was frozen in a liquid nitrogen bath. The NMR tube was evacuated, back filled with D_2 (or ^{13}CO) gas (600 mm Hg) at liquid nitrogen temperature, and slowly warmed up to room temperature. The solution was constantly mixed with the gas ($p \approx 3$ atm) using a mechanical shaker and its ^1H NMR spectrum was periodically recorded. The ratios of isotopomers were calculated from NMR integrations.

Determination of Equilibrium Constants for Alcohol Exchange between Coordinated Alcohols and Free Alcohols. About one equivalent of free alcohol was injected into a solution of alcohol complex in toluene-d_8 (0.03 M) in a Teflon capped NMR tube. The exchange reaction was monitored by ^1H NMR until the equilibrium was reached (typically within 10 min). Equilibria were approached from both directions (Tables 1 and S1, Figures S1 and S2).

Table S1. Dependence of Equilibrium Constant on Alcohol Substituent.

X	σ	-log(K_{eq})(toluene-d_8)	-log(K_{eq}) (CD_2Cl_2)
OCH_3	-0.27	-0.24	-0.17
CH_3	-0.17	-0.13	-0.06
CF_3	0.54	0.49	0.30
NO_2	0.78	0.58	0.46

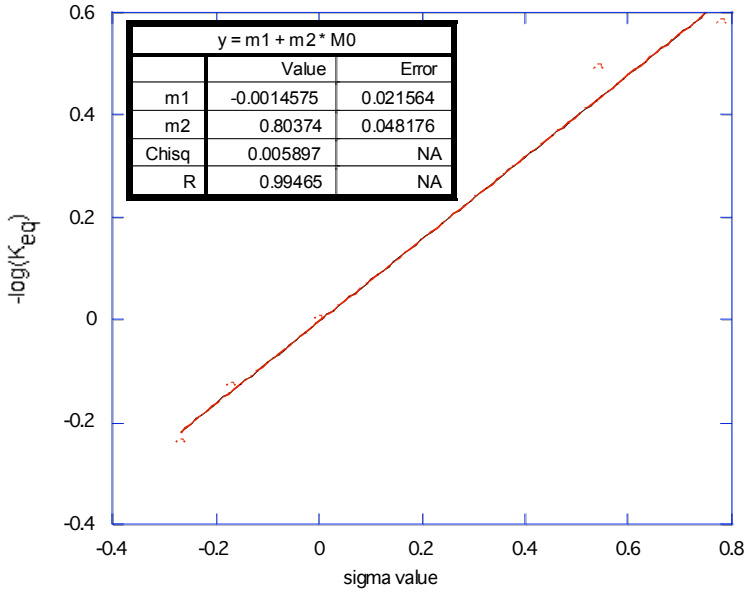

Figure S1. Hammett Plot for Alcohol Complex Equilibria at 25 ºC in Toluene-d_8
ρ (in toluene-d_8) = 0.80(5)

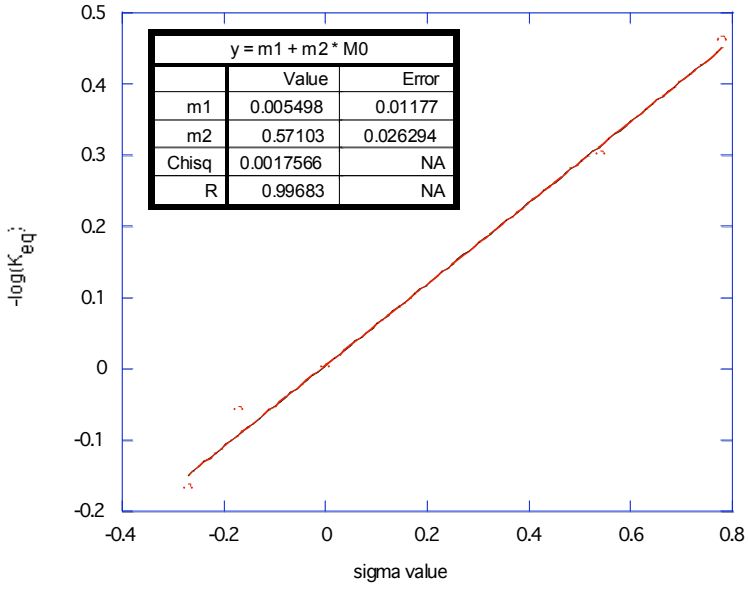

Figure S2. Hammett Plot for Alcohol Complex Equilibria at 25 ºC in CD_2Cl_2
ρ (in CD_2Cl_2) = 0.57(3)

{2,5-(SiMe$_3$)$_2$-3,4-[(CH$_2$)$_4$](η^4-C$_4$CO)}Fe(CO)$_2$(NC$_5$H$_5$) (9) was prepared in 54% yield by a procedure similar to that used for **8**. **9** is not air sensitive, but is moderately light sensitive. ^{1}H NMR ($CDCl_3$, 300 MHz) δ 0.13 (s, Si(CH_3)$_3$, 18H), 1.53-1.72 (m, CH_2, 4H), 2.22-2.44 (m, CH_2, 4H), 7.20-7.25 (m, Ar H, 2H), 7.66-7.73 (m, Ar H, 1H), 8.75-8.78 (m, Ar H, 2H). ^{13}C{^{1}H} NMR ($CDCl_3$, 90 MHz) δ 0.36 (Si(CH_3)$_3$), 22.52 (CH_2), 25.00 (CH_2), 71.15, 105.20, 124.79 (CH), 137.23 (CH), 155.98 (CH), 177.68 (C=O), 214.71 (Fe(CO)$_2$). IR (CH_2Cl_2) 1991, 1929 cm^{-1}. HRMS (ESI) calcd (found) for [$C_{22}H_{31}NO_3FeSi_2$+H]$^+$ 468.1317 (468.1303).

NMR Measurements of Rate of Substitution of Coordinated Alcohols by PhCN and by PPh$_3$. PhCN (or a solution of PPh_3 in toluene-d_8) was added to a solution of alcohol complex **6-H** (0.030 M) and mesitylene (internal standard) in toluene-d_8 in a resealable NMR tube at –78 ºC under a nitrogen atmosphere. The first ^{1}H NMR spectrum was recorded within 5 min of mixing, and the reaction was monitored for three to five half-lives. The height of the Si(CH_3)$_3$ resonance of **6-H** was compared to that of mesitylene (δ 2.15). Zero-filling was used to ensure adequate digital resolution. The NMR probe temperature was calibrated using a 100 % methanol standard.[8] The results are summarized in Tables 2, S2-S12 and Figures 3-4, S3-S6.

Table S2. Rate of Substitution of the Coordinated Alcohol in **6-H** by PhCN in toluene-d_8 at 5 ºC. [a]

[**6-H**]$_0$ (M)	[PhCN]$_0$ (M)	k_{obsd} (s^{-1})
0.030	0.060	3.4×10^{-3}
0.030	0.12	4.1×10^{-3}
0.029	0.23	4.8×10^{-3}
0.029	0.35	4.6×10^{-3}
0.028	0.56	4.7×10^{-3}

[a] For a plot, see Figure 3.

Table S3. Effect of Added Benzyl Alcohol on the Alcohol Substitution Rate for **6-H** in toluene-d_8 at 5 ºC. [a]

$[\mathbf{6\text{-}H}]_0$ (M)	$[PhCH_2OH]_0$ (M)	$[PhCN]_0$ (M)	k_{obsd} (s^{-1})
0.029	0.00	0.35	4.7×10^{-3}
0.029	0.058	0.35	2.8×10^{-3}
0.028	0.11	0.35	1.8×10^{-3}
0.029	0.23	0.35	1.1×10^{-3}

[a] For a plot, see Figure 4.

Table S4. Rate of Substitution of the Coordinated Alcohol in **6-H** by PhCN in toluene-d_8 at Other Temperatures.

T (ºC)	[**6-H**]$_0$ (M)	[PhCN]$_0$ (M)	k_{obsd} (s^{-1})
–1.4	0.029	0.35	2.4×10^{-3}
–1.4	0.028	0.56	2.5×10^{-3}
–5.3	0.029	0.35	1.4×10^{-3}
–5.3	0.028	0.56	1.6×10^{-3}
–5.3	0.027	0.82	1.6×10^{-3}
–10.3	0.028	0.56	8.2×10^{-4}
–10.3	0.027	0.82	8.4×10^{-4}

Table S5. Summary of Dissociation Rate for **6-H** in Toluene-d_8 at Various Temperatures.

T (K)	K_{obsd} (s^{-1})	1/T (K^{-1})	ln(k_{obsd}/T)
278.2	4.7×10^{-3}	0.00359	−10.99
271.8	2.5×10^{-3}	0.00368	−11.60
267.9	1.6×10^{-3}	0.00373	−12.03
262.9	8.4×10^{-4}	0.00380	−12.65

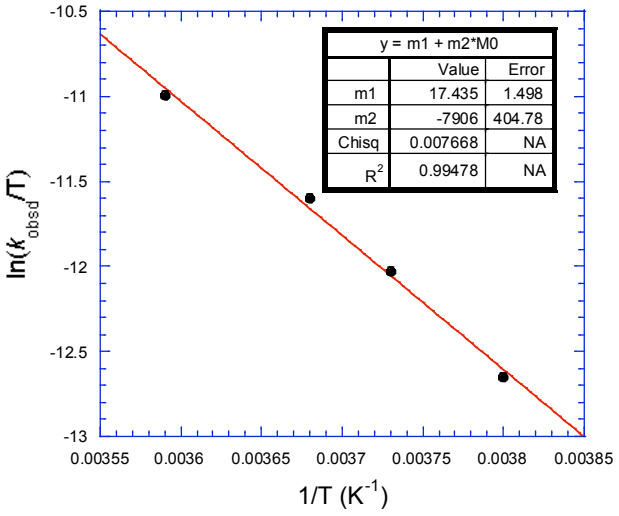

Figure S3. Eyring Plot for Alcohol Dissociation from **6-H** in Toluene-d_8

$\Delta H^{\ddagger} = 15.7 \pm 0.8$ kcal mol^{-1} and $\Delta S^{\ddagger} = -12.6 \pm 3.0$ cal deg^{-1} mol^{-1}

Table S6. Rate of Substitution of the Coordinated Alcohol in **6-CH$_3$** by PhCN in toluene-d_8 at Various Temperatures.

T (ºC)	[**6-CH$_3$**]$_0$ (M)	[PhCN]$_0$ (M)	k_{obsd} (s^{-1})
9.0	0.029	0.23	6.2×10^{-3}
9.0	0.028	0.56	6.3×10^{-3}
5.0	0.029	0.23	3.9×10^{-3}
5.0	0.028	0.56	3.9×10^{-3}
–1.4	0.028	0.56	2.1×10^{-3}
–1.4	0.027	0.82	2.2×10^{-3}
–5.3	0.027	0.82	1.1×10^{-3}
–5.3	0.027	1.07	1.2×10^{-3}

Table S7. Summary of Dissociation Rate for **6-CH$_3$** in Toluene-d_8 at Various Temperatures.

T (K)	k_{obsd} (s^{-1})	1/T (K^{-1})	ln(k_{obsd}/T)
282.2	6.3×10^{-3}	0.00354	−10.71
278.2	3.9×10^{-3}	0.00359	−11.18
271.8	2.2×10^{-3}	0.00368	−11.72
267.9	1.2×10^{-3}	0.00373	−12.32

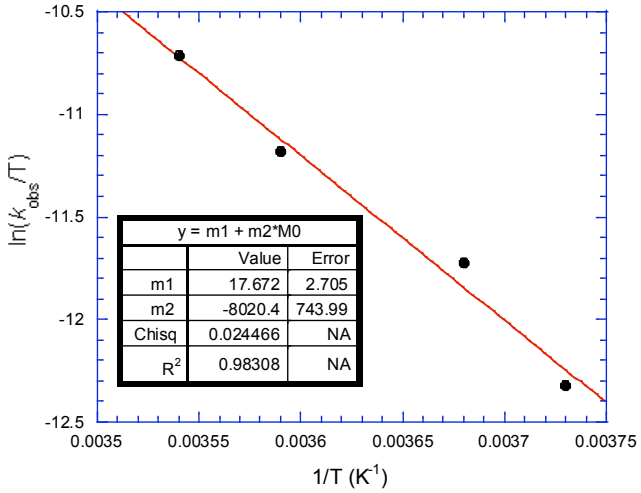

Figure S4. Eyring Plot for Alcohol Dissociation from **6-CH$_3$** in toluene-d_8

$\Delta H^{\ddagger} = 15.9 \pm 1.5$ kcal mol^{-1} and $\Delta S^{\ddagger} = -13.2 \pm 5.4$ cal deg^{-1} mol^{-1}

Table S8. Rate for Substitution of the Coordinated Alcohol in **6-NO$_2$** by PhCN in toluene-d_8 at Various Temperatures.

T (ºC)	[**6-NO$_2$**]$_0$ (M)	[PhCN]$_0$ (M)	k_{obsd} (s^{-1})
5.0	0.029	0.23	2.1×10^{-2}
5.0	0.029	0.35	2.0×10^{-2}
–1.4	0.029	0.23	1.1×10^{-2}
–1.4	0.029	0.35	1.2×10^{-2}
–5.3	0.029	0.35	8.2×10^{-3}
–5.3	0.028	0.56	8.4×10^{-3}
–10.9	0.029	0.35	4.0×10^{-3}
–10.3	0.028	0.56	4.1×10^{-3}

Table S9. Summary of Dissociation Rate for **6-NO$_2$** in Toluene-d_8 at Various Temperatures.

T (K)	K_{obsd} (s^{-1})	1/T (K^{-1})	ln(k_{obsd}/T)
278.2	2.0×10^{-2}	0.00359	–9.54
271.8	1.2×10^{-2}	0.00368	–10.03
267.9	8.3×10^{-3}	0.00373	–10.38
262.3	4.1×10^{-3}	0.00381	–11.07

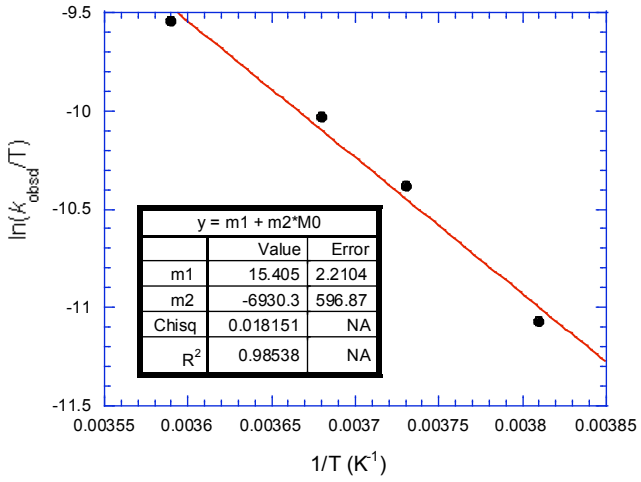

Figure S5. Eyring Plot for Alcohol Dissociation from **6-NO$_2$** in Toluene-d_8

$\Delta H^{\ddagger} = 13.8 \pm 1.2$ kcal mol^{-1} and $\Delta S^{\ddagger} = -16.6 \pm 4.4$ cal deg^{-1} mol^{-1}

Table S10. Rate of Substitution of the Coordinated Alcohols in **6-OCH$_3$** and **6-CF$_3$** by PhCN in toluene-d_8 at 5 ºC.

[**6-OCH$_3$**]$_0$ (M)	[**6-CF$_3$**]$_0$ (M)	[PhCN]$_0$ (M)	k_{obsd} (s^{-1})
0.029		0.35	2.1×10^{-3}
0.028		0.56	2.2×10^{-3}
	0.029	0.23	1.5×10^{-2}
	0.028	0.56	1.6×10^{-2}

Table S11. Dependence of Rate of Alcohol Substitution on Alcohol Substituent.

Alcohol Complex	σ	$\log(k_X/k_H)$
6-OCH$_3$	-0.27	-0.33
6-CH$_3$	-0.17	-0.08
6-H	0.0	0
6-CF$_3$	0.54	0.53
6-NO$_2$	0.78	0.63

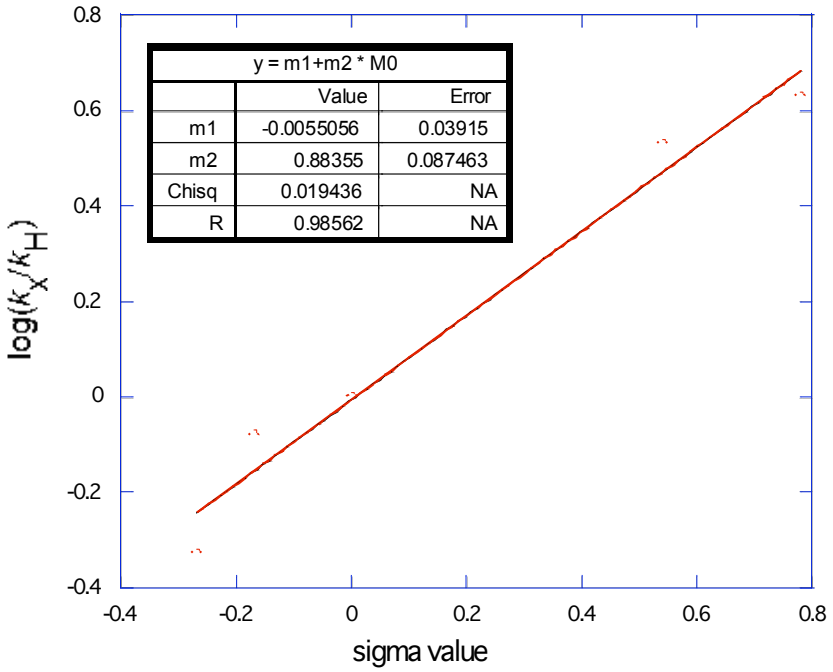

Figure S6. Hammett Plot of Alcohol Substitution Rate at 5 ºC in Toluene-d_8
ρ = 0.88(9)

Table S12. Rate for Substitution of the Coordinated Alcohol in **6-H** by PPh_3 in toluene-d_8 at 5 ºC. [a]

$[\mathbf{6\text{-}H}]_0$ (M)	$[PPh_3]_0$ (M)	k_{obsd} (s^{-1})
0.024	0.048	9.6×10^{-4}
0.024	0.096	1.7×10^{-3}
0.024	0.14	2.3×10^{-3}
0.024	0.19	2.9×10^{-3}

[a] For a plot, see Figure 3.

Attempted Kinetic Study of Reaction of H_2 with 6-CH_3 by IR. An attempt to measure the rate of reaction of alcohol complexes with H_2 was made using a high-pressure vessel equipped with an attenuated total reflectance IR apparatus.[9] The CO stretching frequencies of alcohol complexes **6-H** were too close to those of hydride **3** to permit monitoring the reaction by IR. However, it was possible to monitor the disappearance of **6-CH_3** (2012 and 1959 cm^{-1}) and appearance of **3** (2001 and 1941 cm^{-1}). A solution of **6-CH_3** (generated *in situ* from **3** and 4-tolualdehyde) in toluene was rapidly stirred and then the system was opened to 21 atm of H_2 at 25 °C. The IR spectrum of the resulting reaction mixture was taken after one minute and showed complete reaction.

Kinetics of the Hydrogenation of Aldehydes Catalyzed by 3. Hydrogenations were performed in a 25 mL stainless steel Parr reactor equipped with a magnetic drive stirrer, a Parr 4842 thermocouple, and a ReactIR SiComp cell. A solution of **3** in toluene was loaded into the reactor and a solution of the aldehyde was loaded into a stainless steel addition funnel under a nitrogen atmosphere in a glove box. The reactor assembly was then connected to a hydrogen source and the atmosphere in the reactor was switched to H_2 by several cycles of pressurizing to 100 psi H_2 and then releasing the pressure, all the while stirring rapidly. Then the material in the addition funnel was placed under higher pressure of H_2 and the injection valve opened to flush

the aldehyde solution into the reactor and the higher pressure was maintained throughout the hydrogenation. The IR spectra of the resulting reaction mixture were collected using an ASI Applied Systems ReactIR 1000 FTIR. The disappearance of aldehyde ($\nu_{C=O}$ 1708 cm^{-1}) was monitored as a function of time. Reaction data were imported into Excel and processed in KaleidaGraph. The results are summarized in Tables S13-S14 and Figure S7-8.

Table S13. Rate of Hydrogenation of PhCHO catalyzed by **3** in toluene at 25 °C.

$[\mathbf{3}]_0$ (M)	$[PhCHO]_0$ (M)	$p(H_2)$ (atm)	k_{obsd} (s^{-1})
0.0054	0.50	35	3.0×10^{-4}
0.010	0.50	35	6.4×10^{-4}
0.015	0.50	35	1.4×10^{-3}
0.015	0.50	21	1.4×10^{-3}
0.020	0.50	35	1.9×10^{-3}
0.021	0.50	35	2.2×10^{-3}

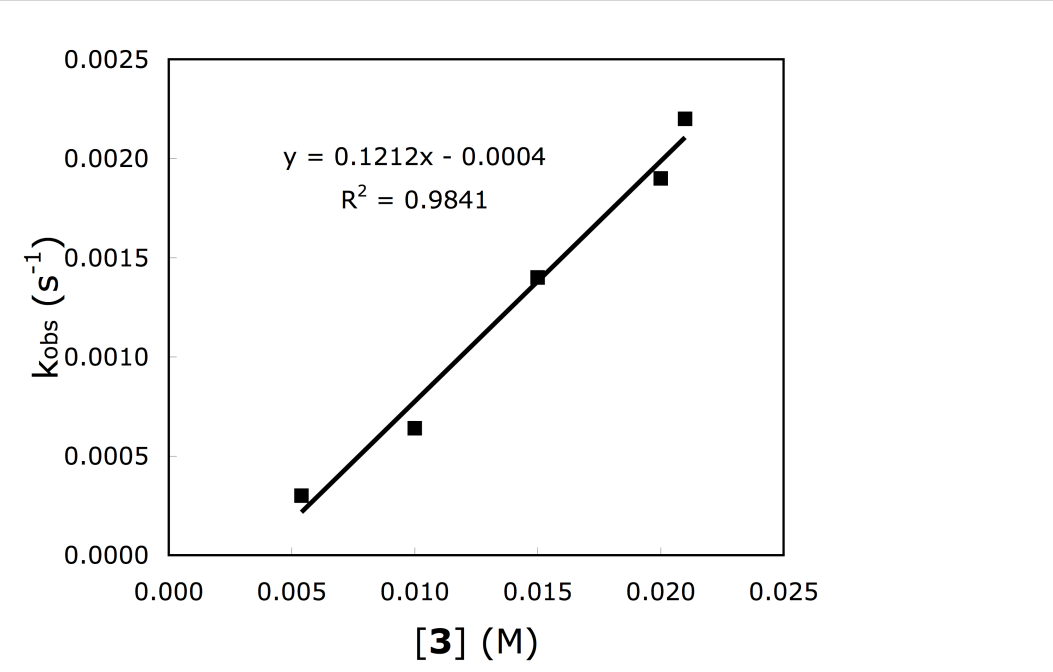

Figure S7. Plot of Observed Rate versus Concentration of **3** for the Hydrogenation of PhCHO in Toluene at 25 °C

Table S14. Rate of Hydrogenation of TolCHO catalyzed by **3** in toluene at 25 °C.

$[\mathbf{3}]_0$ (M)	$[\text{TolCHO}]_0$ (M)	$p(H_2)$ (atm)	k_{obsd} (s^{-1})
0.0050	0.50	35	5.4×10^{-4}
0.010	0.50	35	1.2×10^{-3}
0.015	0.50	35	1.6×10^{-3}
0.020	0.50	35	2.0×10^{-3}

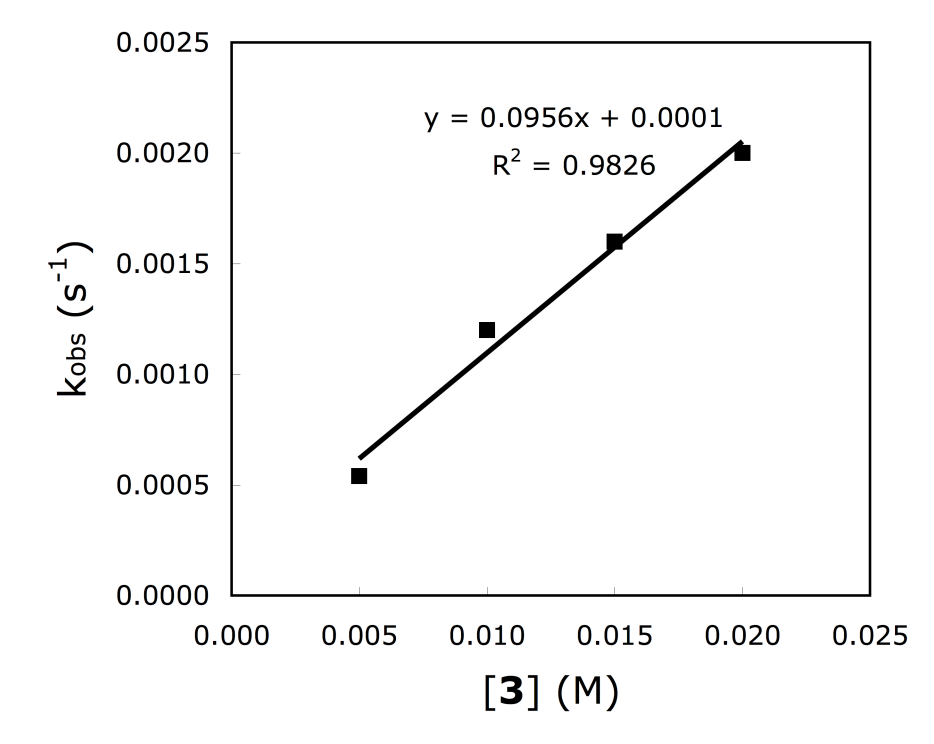

Figure S8. Plot of Observed Rate versus Concentration of **3** for the Hydrogenation of 4-Tolualdehyde in Toluene at 25 °C

X-Ray Crystallographic Determination of {2,5-$(SiMe_3)_2$-3,4-$[(CH_2)_4]$(η^4-C_4CO)}$Fe(CO)_2(C_6H_5CH_2OH)$ (6-H). An orange crystal of **6-H** with approximate dimensions 0.37 x 0.32 x 0.24 mm^3 was selected under oil under ambient conditions and attached to the tip of a Micromount©. The crystal was mounted in a stream of cold nitrogen at 105(2) K and centered in the X-ray beam by using a video camera.

The crystal evaluation and data collection were performed on a Bruker CCD-1000 diffractometer with Mo K_α (λ = 0.71073 Å) radiation and the diffractometer to crystal distance of 4.9 cm. The initial cell constants were obtained from three series of ω scans at different starting angles. Each series consisted of 20 frames collected at intervals of 0.3º in a 6º range about ω with the exposure time of 6 seconds per frame. The reflections were successfully indexed by an automated indexing routine built in the SMART program. The final cell constants were calculated from a set of 16940 strong reflections from the actual data collection. The data were collected by using the full sphere data collection routine to survey the reciprocal space to the extent of a full sphere to a resolution of 0.80 Å. A total of 43844 data were harvested by collecting four sets of frames with 0.3º scans in ω and one set with 0.4º scans in ϕ with an exposure time 16 sec per frame. These highly redundant datasets were corrected for Lorentz and polarization effects. The absorption correction was based on fitting a function to the empirical transmission surface as sampled by multiple equivalent measurements.[10] The systematic absences in the diffraction data were consistent for the space groups *Cc* and *C2/c*. The *E*-statistics strongly suggested the centrosymmetric space group *C2/c* that yielded chemically reasonable and computationally stable results of refinement.[10] A successful solution by the direct methods provided most non-hydrogen atoms from the *E*-map. The remaining non-hydrogen atoms were located in an alternating series of least-squares cycles and difference Fourier maps. All non-hydrogen atoms were refined with anisotropic displacement coefficients. All hydrogen atoms except H2 were included in the structure factor calculation at idealized positions and were allowed to ride on the neighboring atoms with relative isotropic displacement coefficients. Atom H2 was located in the difference map and refined independently with a restrained O2-H2 distance. The final least-squares refinement of 290 parameters against 6768 data resulted in residuals *R* (based on F^2 for $I \geq 2\sigma$) and *wR* (based on F^2 for all data) of 0.0308 and 0.0857, respectively. The final difference Fourier map was featureless.

Table S15. Crystal data and structure refinement for **6-H**.

Empirical formula	$C_{24}\ H_{34}\ Fe\ O_4\ Si_2$	
Formula weight	498.54	
Temperature	105(2) K	
Wavelength	0.71073 Å	
Crystal system	Monoclinic	
Space group	C2/c	
Unit cell dimensions	a = 18.7736(13) Å	α= 90°.
	b = 10.6759(7) Å	β= 109.6210(10)°.
	c = 26.9091(19) Å	γ = 90°.
Volume	5080.1(6) $Å^3$	
Z	8	
Density (calculated)	1.304 Mg/m^3	
Absorption coefficient	0.715 mm^{-1}	
F(000)	2112	
Crystal size	0.37 x 0.32 x 0.24 mm^3	
Theta range for data collection	2.23 to 29.13°.	
Index ranges	-25<=h<=25, -14<=k<=14, -36<=l<=36	
Reflections collected	43844	
Independent reflections	6768 [R(int) = 0.0319]	
Completeness to theta = 29.13°	98.8 %	
Absorption correction	Empirical with SADABS	
Max. and min. transmission	0.8472 and 0.7780	
Refinement method	Full-matrix least-squares on F^2	
Data / restraints / parameters	6768 / 1 / 290	
Goodness-of-fit on F^2	1.064	
Final R indices [I>2sigma(I)]	R1 = 0.0308, wR2 = 0.0804	
R indices (all data)	R1 = 0.0387, wR2 = 0.0857	
Largest diff. peak and hole	0.664 and -0.208 $e.Å^{-3}$	

Table S16. Atomic coordinates (x 10^4) and equivalent isotropic displacement parameters ($Å^2$x 10^3) for **6-H**. U(eq) is defined as one third of the trace of the orthogonalized U^{ij} tensor.

	x	y	z	U(eq)
Fe(1)	3788(1)	6288(1)	974(1)	15(1)
Si(1)	4050(1)	2922(1)	1122(1)	18(1)
Si(2)	5610(1)	7806(1)	1316(1)	17(1)
O(1)	5234(1)	5210(1)	1795(1)	18(1)
O(2)	3996(1)	6272(1)	1770(1)	19(1)
O(3)	3390(1)	8923(1)	743(1)	30(1)
O(4)	2205(1)	5495(1)	554(1)	30(1)
C(1)	4906(1)	5350(1)	1299(1)	15(1)
C(2)	4310(1)	4531(1)	954(1)	16(1)
C(3)	4064(1)	5116(1)	442(1)	16(1)
C(4)	3547(1)	4573(1)	-72(1)	20(1)
C(5)	3586(1)	5318(1)	-548(1)	26(1)
C(6)	3592(1)	6721(1)	-453(1)	25(1)
C(7)	4312(1)	7107(1)	-6(1)	20(1)
C(8)	4427(1)	6305(1)	474(1)	16(1)
C(9)	4930(1)	6497(1)	1007(1)	16(1)
C(10)	4367(1)	2667(1)	1847(1)	26(1)
C(11)	4531(1)	1752(1)	828(1)	30(1)
C(12)	3009(1)	2637(2)	846(1)	31(1)
C(13)	6569(1)	7104(1)	1620(1)	22(1)
C(14)	5321(1)	8610(1)	1836(1)	25(1)
C(15)	5665(1)	8957(1)	806(1)	25(1)
C(16)	3477(1)	5750(1)	2006(1)	19(1)
C(17)	2847(1)	6659(1)	1962(1)	19(1)
C(18)	2956(1)	7946(1)	1955(1)	23(1)
C(19)	2374(1)	8760(2)	1948(1)	28(1)
C(20)	1686(1)	8297(2)	1955(1)	33(1)
C(21)	1578(1)	7024(2)	1961(1)	32(1)
C(22)	2152(1)	6198(2)	1961(1)	24(1)
C(23)	3540(1)	7898(1)	849(1)	20(1)
C(24)	2822(1)	5808(1)	739(1)	20(1)

Table S17. Bond lengths [Å] and angles [°] for **6-H**.

Fe(1)-C(23)	1.7822(14)	C(7)-H(7A)	0.9900
Fe(1)-C(24)	1.7840(14)	C(7)-H(7B)	0.9900
Fe(1)-O(2)	2.0442(10)	C(8)-C(9)	1.4424(18)
Fe(1)-C(8)	2.0813(13)	C(10)-H(10A)	0.9800
Fe(1)-C(3)	2.0924(13)	C(10)-H(10B)	0.9800
Fe(1)-C(2)	2.1255(13)	C(10)-H(10C)	0.9800
Fe(1)-C(9)	2.1263(13)	C(11)-H(11A)	0.9800
Fe(1)-C(1)	2.2221(12)	C(11)-H(11B)	0.9800
Si(1)-C(10)	1.8581(15)	C(11)-H(11C)	0.9800
Si(1)-C(11)	1.8656(15)	C(12)-H(12A)	0.9800
Si(1)-C(12)	1.8681(16)	C(12)-H(12B)	0.9800
Si(1)-C(2)	1.8815(13)	C(12)-H(12C)	0.9800
Si(2)-C(13)	1.8665(14)	C(13)-H(13A)	0.9800
Si(2)-C(15)	1.8706(15)	C(13)-H(13B)	0.9800
Si(2)-C(14)	1.8699(15)	C(13)-H(13C)	0.9800
Si(2)-C(9)	1.8864(13)	C(14)-H(14A)	0.9800
O(1)-C(1)	1.2768(16)	C(14)-H(14B)	0.9800
O(2)-C(16)	1.4432(16)	C(14)-H(14C)	0.9800
O(2)-H(2)	0.832(9)	C(15)-H(15A)	0.9800
O(3)-C(23)	1.1425(17)	C(15)-H(15B)	0.9800
O(4)-C(24)	1.1469(17)	C(15)-H(15C)	0.9800
C(1)-C(9)	1.4641(18)	C(16)-C(17)	1.5030(18)
C(1)-C(2)	1.4766(18)	C(16)-H(16A)	0.9900
C(2)-C(3)	1.4401(18)	C(16)-H(16B)	0.9900
C(3)-C(8)	1.4303(18)	C(17)-C(18)	1.390(2)
C(3)-C(4)	1.5135(18)	C(17)-C(22)	1.394(2)
C(4)-C(5)	1.5304(19)	C(18)-C(19)	1.392(2)
C(4)-H(4A)	0.9900	C(18)-H(18)	0.9500
C(4)-H(4B)	0.9900	C(19)-C(20)	1.388(3)
C(5)-C(6)	1.519(2)	C(19)-H(19)	0.9500
C(5)-H(5A)	0.9900	C(20)-C(21)	1.375(3)
C(5)-H(5B)	0.9900	C(20)-H(20)	0.9500
C(6)-C(7)	1.533(2)	C(21)-C(22)	1.391(2)
C(6)-H(6A)	0.9900	C(21)-H(21)	0.9500
C(6)-H(6B)	0.9900	C(22)-H(22)	0.9500
C(7)-C(8)	1.5029(18)		

C(23)-Fe(1)-C(24)	92.29(6)	C(24)-Fe(1)-C(3)	92.40(6)
C(23)-Fe(1)-O(2)	98.72(5)	O(2)-Fe(1)-C(3)	135.01(5)
C(24)-Fe(1)-O(2)	100.46(5)	C(8)-Fe(1)-C(3)	40.08(5)
C(23)-Fe(1)-C(8)	92.34(6)	C(23)-Fe(1)-C(2)	160.02(6)
C(24)-Fe(1)-C(8)	120.82(6)	C(24)-Fe(1)-C(2)	99.18(6)
O(2)-Fe(1)-C(8)	136.76(5)	O(2)-Fe(1)-C(2)	95.23(4)
C(23)-Fe(1)-C(3)	123.83(6)	C(8)-Fe(1)-C(2)	67.74(5)

C(3)-Fe(1)-C(2)	39.92(5)	C(4)-C(3)-Fe(1)	128.60(9)
C(23)-Fe(1)-C(9)	95.93(6)	C(3)-C(4)-C(5)	111.70(11)
C(24)-Fe(1)-C(9)	159.34(6)	C(3)-C(4)-H(4A)	109.3
O(2)-Fe(1)-C(9)	96.99(4)	C(5)-C(4)-H(4A)	109.3
C(8)-Fe(1)-C(9)	40.08(5)	C(3)-C(4)-H(4B)	109.3
C(3)-Fe(1)-C(9)	67.31(5)	C(5)-C(4)-H(4B)	109.3
C(2)-Fe(1)-C(9)	68.12(5)	H(4A)-C(4)-H(4B)	107.9
C(23)-Fe(1)-C(1)	131.43(6)	C(6)-C(5)-C(4)	111.81(12)
C(24)-Fe(1)-C(1)	136.29(6)	C(6)-C(5)-H(5A)	109.3
O(2)-Fe(1)-C(1)	76.15(4)	C(4)-C(5)-H(5A)	109.3
C(8)-Fe(1)-C(1)	65.53(5)	C(6)-C(5)-H(5B)	109.3
C(3)-Fe(1)-C(1)	65.30(5)	C(4)-C(5)-H(5B)	109.3
C(2)-Fe(1)-C(1)	39.63(5)	H(5A)-C(5)-H(5B)	107.9
C(9)-Fe(1)-C(1)	39.27(5)	C(5)-C(6)-C(7)	110.63(12)
C(10)-Si(1)-C(11)	108.45(7)	C(5)-C(6)-H(6A)	109.5
C(10)-Si(1)-C(12)	108.48(7)	C(7)-C(6)-H(6A)	109.5
C(11)-Si(1)-C(12)	108.24(8)	C(5)-C(6)-H(6B)	109.5
C(10)-Si(1)-C(2)	111.64(6)	C(7)-C(6)-H(6B)	109.5
C(11)-Si(1)-C(2)	107.90(6)	H(6A)-C(6)-H(6B)	108.1
C(12)-Si(1)-C(2)	112.01(7)	C(8)-C(7)-C(6)	110.86(11)
C(13)-Si(2)-C(15)	107.60(7)	C(8)-C(7)-H(7A)	109.5
C(13)-Si(2)-C(14)	109.58(7)	C(6)-C(7)-H(7A)	109.5
C(15)-Si(2)-C(14)	110.38(7)	C(8)-C(7)-H(7B)	109.5
C(13)-Si(2)-C(9)	107.85(6)	C(6)-C(7)-H(7B)	109.5
C(15)-Si(2)-C(9)	111.07(6)	H(7A)-C(7)-H(7B)	108.1
C(14)-Si(2)-C(9)	110.28(6)	C(3)-C(8)-C(9)	108.96(11)
C(16)-O(2)-Fe(1)	123.04(8)	C(3)-C(8)-C(7)	121.74(12)
C(16)-O(2)-H(2)	106.4(16)	C(9)-C(8)-C(7)	129.12(12)
Fe(1)-O(2)-H(2)	105.3(16)	C(3)-C(8)-Fe(1)	70.38(7)
O(1)-C(1)-C(9)	124.62(12)	C(9)-C(8)-Fe(1)	71.64(7)
O(1)-C(1)-C(2)	125.81(12)	C(7)-C(8)-Fe(1)	127.71(9)
C(9)-C(1)-C(2)	108.14(11)	C(8)-C(9)-C(1)	106.70(11)
O(1)-C(1)-Fe(1)	121.63(9)	C(8)-C(9)-Si(2)	131.53(10)
C(9)-C(1)-Fe(1)	66.83(7)	C(1)-C(9)-Si(2)	121.41(9)
C(2)-C(1)-Fe(1)	66.66(7)	C(8)-C(9)-Fe(1)	68.28(7)
C(3)-C(2)-C(1)	106.04(11)	C(1)-C(9)-Fe(1)	73.90(7)
C(3)-C(2)-Si(1)	126.88(10)	Si(2)-C(9)-Fe(1)	128.25(7)
C(1)-C(2)-Si(1)	126.32(10)	Si(1)-C(10)-H(10A)	109.5
C(3)-C(2)-Fe(1)	68.80(7)	Si(1)-C(10)-H(10B)	109.5
C(1)-C(2)-Fe(1)	73.71(7)	H(10A)-C(10)-H(10B)	109.5
Si(1)-C(2)-Fe(1)	129.85(7)	Si(1)-C(10)-H(10C)	109.5
C(8)-C(3)-C(2)	109.55(11)	H(10A)-C(10)-H(10C)	109.5
C(8)-C(3)-C(4)	122.77(12)	H(10B)-C(10)-H(10C)	109.5
C(2)-C(3)-C(4)	127.56(12)	Si(1)-C(11)-H(11A)	109.5
C(8)-C(3)-Fe(1)	69.54(7)	Si(1)-C(11)-H(11B)	109.5
C(2)-C(3)-Fe(1)	71.28(7)	H(11A)-C(11)-H(11B)	109.5

Si(1)-C(11)-H(11C)	109.5	O(2)-C(16)-C(17)	110.28(11)
H(11A)-C(11)-H(11C)	109.5	O(2)-C(16)-H(16A)	109.6
H(11B)-C(11)-H(11C)	109.5	C(17)-C(16)-H(16A)	109.6
Si(1)-C(12)-H(12A)	109.5	O(2)-C(16)-H(16B)	109.6
Si(1)-C(12)-H(12B)	109.5	C(17)-C(16)-H(16B)	109.6
H(12A)-C(12)-H(12B)	109.5	H(16A)-C(16)-H(16B)	108.1
Si(1)-C(12)-H(12C)	109.5	C(18)-C(17)-C(22)	119.42(13)
H(12A)-C(12)-H(12C)	109.5	C(18)-C(17)-C(16)	121.56(13)
H(12B)-C(12)-H(12C)	109.5	C(22)-C(17)-C(16)	118.91(13)
Si(2)-C(13)-H(13A)	109.5	C(17)-C(18)-C(19)	119.92(14)
Si(2)-C(13)-H(13B)	109.5	C(17)-C(18)-H(18)	120.0
H(13A)-C(13)-H(13B)	109.5	C(19)-C(18)-H(18)	120.0
Si(2)-C(13)-H(13C)	109.5	C(20)-C(19)-C(18)	120.43(15)
H(13A)-C(13)-H(13C)	109.5	C(20)-C(19)-H(19)	119.8
H(13B)-C(13)-H(13C)	109.5	C(18)-C(19)-H(19)	119.8
Si(2)-C(14)-H(14A)	109.5	C(21)-C(20)-C(19)	119.62(14)
Si(2)-C(14)-H(14B)	109.5	C(21)-C(20)-H(20)	120.2
H(14A)-C(14)-H(14B)	109.5	C(19)-C(20)-H(20)	120.2
Si(2)-C(14)-H(14C)	109.5	C(20)-C(21)-C(22)	120.58(15)
H(14A)-C(14)-H(14C)	109.5	C(20)-C(21)-H(21)	119.7
H(14B)-C(14)-H(14C)	109.5	C(22)-C(21)-H(21)	119.7
Si(2)-C(15)-H(15A)	109.5	C(21)-C(22)-C(17)	120.02(15)
Si(2)-C(15)-H(15B)	109.5	C(21)-C(22)-H(22)	120.0
H(15A)-C(15)-H(15B)	109.5	C(17)-C(22)-H(22)	120.0
Si(2)-C(15)-H(15C)	109.5	O(3)-C(23)-Fe(1)	176.19(13)
H(15A)-C(15)-H(15C)	109.5	O(4)-C(24)-Fe(1)	175.17(13)
H(15B)-C(15)-H(15C)	109.5		

Table S18. Anisotropic displacement parameters ($Å^2 x\ 10^3$)for **6-H**. The anisotropic displacement factor exponent takes the form: $-2p^2[\ h^2 a^{*2} U^{11} + ... + 2\ h\ k\ a^*\ b^*\ U^{12}\ ]$

	U^{11}	U^{22}	U^{33}	U^{23}	U^{13}	U^{12}
Fe(1)	12(1)	16(1)	16(1)	0(1)	4(1)	2(1)
Si(1)	19(1)	16(1)	19(1)	0(1)	7(1)	-1(1)
Si(2)	15(1)	17(1)	19(1)	-2(1)	6(1)	-1(1)
O(1)	13(1)	22(1)	16(1)	1(1)	3(1)	3(1)
O(2)	14(1)	26(1)	18(1)	2(1)	6(1)	4(1)
O(3)	30(1)	21(1)	38(1)	5(1)	10(1)	6(1)
O(4)	15(1)	36(1)	35(1)	0(1)	5(1)	-1(1)
C(1)	12(1)	17(1)	18(1)	-1(1)	6(1)	2(1)
C(2)	14(1)	16(1)	18(1)	-1(1)	6(1)	1(1)
C(3)	14(1)	18(1)	17(1)	-1(1)	6(1)	2(1)
C(4)	20(1)	20(1)	18(1)	-2(1)	5(1)	-2(1)
C(5)	30(1)	28(1)	18(1)	-1(1)	6(1)	-1(1)
C(6)	26(1)	27(1)	20(1)	3(1)	5(1)	1(1)
C(7)	21(1)	21(1)	18(1)	2(1)	7(1)	-1(1)
C(8)	14(1)	18(1)	16(1)	0(1)	6(1)	1(1)
C(9)	13(1)	17(1)	18(1)	-1(1)	6(1)	1(1)
C(10)	30(1)	24(1)	22(1)	4(1)	10(1)	2(1)
C(11)	47(1)	18(1)	35(1)	0(1)	24(1)	1(1)
C(12)	25(1)	32(1)	33(1)	6(1)	5(1)	-9(1)
C(13)	17(1)	24(1)	25(1)	-3(1)	6(1)	-2(1)
C(14)	24(1)	26(1)	26(1)	-8(1)	9(1)	-3(1)
C(15)	29(1)	21(1)	26(1)	0(1)	10(1)	-5(1)
C(16)	18(1)	23(1)	21(1)	4(1)	10(1)	6(1)
C(17)	17(1)	25(1)	14(1)	0(1)	5(1)	7(1)
C(18)	24(1)	25(1)	18(1)	-1(1)	6(1)	4(1)
C(19)	37(1)	26(1)	20(1)	-1(1)	7(1)	13(1)
C(20)	28(1)	46(1)	24(1)	-1(1)	7(1)	21(1)
C(21)	18(1)	49(1)	29(1)	1(1)	9(1)	9(1)
C(22)	19(1)	30(1)	23(1)	1(1)	8(1)	3(1)
C(23)	15(1)	24(1)	21(1)	-1(1)	6(1)	2(1)
C(24)	18(1)	22(1)	22(1)	2(1)	9(1)	3(1)

Table S19. Hydrogen coordinates (x 10^4) and isotropic displacement parameters (Å^{2}x 10^3) for **6-H**.

	x	y	z	U(eq)
H(2)	4401(8)	5880(20)	1897(8)	50(6)
H(4A)	3020	4577	-71	24
H(4B)	3692	3693	-103	24
H(5A)	4049	5080	-623	31
H(5B)	3145	5102	-861	31
H(6A)	3143	6957	-360	30
H(6B)	3567	7172	-780	30
H(7A)	4754	7023	-126	24
H(7B)	4272	7996	86	24
H(10A)	4084	3221	2003	38
H(10B)	4908	2852	2000	38
H(10C)	4276	1793	1920	38
H(11A)	5077	1907	958	46
H(11B)	4338	1829	443	46
H(11C)	4430	906	929	46
H(12A)	2904	1757	899	46
H(12B)	2826	2827	468	46
H(12C)	2750	3176	1026	46
H(13A)	6918	7743	1827	33
H(13B)	6750	6791	1342	33
H(13C)	6541	6410	1851	33
H(14A)	5298	7997	2101	38
H(14B)	4822	8993	1674	38
H(14C)	5691	9261	2004	38
H(15A)	6030	9615	975	37
H(15B)	5166	9333	635	37
H(15C)	5828	8527	541	37
H(16A)	3749	5560	2382	23
H(16B)	3264	4958	1825	23
H(18)	3427	8269	1954	27
H(19)	2448	9639	1940	34
H(20)	1292	8855	1954	39
H(21)	1108	6705	1965	38
H(22)	2069	5320	1959	29

Table S20. Hydrogen bonds for **6-H** [Å and °].

D-H···A	d(D-H)	d(H···A)	d(D···A)	<(DHA)
O(2)-H(2)···O(1)	0.832(9)	1.824(15)	2.5652(13)	148(2)

References

(1) Pangborn, A. B.; Giardello, M. A.; Grubbs, R. H.; Rosen, R. K.; Timmers, F. J. *Organometallics* **1996**, *15*, 1518.

(2) Knölker, H.-J.; Baum, E.; Goesmann, H.; Klauss, R. *Angew. Chem. Int. Ed.* **1999**, *38*, 2064.

(3) Pearson, A. J.; Shively, R. J., Jr.; Dubbert, R. A. *Organometallics* **1992**, *11*, 4096.

(4) Mak, C. C.; Bampos, N.; Darling, S. L.; Montalti, M.; Prodi, L.; Sanders, J. K. M. *J. Org. Chem.* **2001**, *66*, 4476.

(5) Roberts, S. L.; Furlan, R. L. E.; Otto, S.; Sanders, J. K. M. *Org. Biomol. Chem.* **2003**, *1*, 1625.

(6) The solution of **6-NO$_2$** in toluene-d_8 had a deep purple color.

(7) The reaction and purification procedures were similar as those reported for **3**.

(8) (a) van Geet, A. L. *Anal. Chem.* **1970**, *42*, 679. (b) Raidford, D. S.; Fisk, C. L.; Becker, E. D. *Anal. Chem.* **1979**, *51*, 2050.

(9) The CO stretching frequencies of alcohol complexes **6-H**, **6-OCH$_3$**, **6-NO$_2$**, and **6-CF$_3$** were too close to those of hydride **3** to enable monitoring the reaction by IR.

(10) Bruker-AXS. (2000-2003) SADABS V.2.05, SAINT V.6.22, SHELXTL V.6.10 & SMART 5.622 Software Reference Manuals. Bruker-AXS, Madison, Wisconsin, USA.